World Journal of Condensed Matter Physics, 2026, 16(3), 73-89
https://www.scirp.org/journal/wjcmp
ISSN Online: 2160-6927
ISSN Print: 2160-6919

Thermophysical Properties of InTl Melts at 723 K

Rajendra Prasad Chaudhary[1], Md. Mosarrat Hussain[2], Nabin Kumar Roy[3], Jagdhar Mandal[4*], Indu Shekhar Jha[1]

[1]Department of Physics, M.M.A.M. Campus, Biratnagar, T.U., Nepal
[2]G.B. College, Naugachia, Under T.M. Bhagalpur University, Bhagalpur, India
[3]University Department of Chemistry, T.M. Bhagalpur University, Bhagalpur, India
[4]University Department of Physics, T.M. Bhagalpur University, Bhagalpur, India
Email: r.p.chaudhary028@gmail.com, mossarathussain15@gmail.com, nabinkrroy@gmail.com, *jmandal1284@gmail.com, isjha12345@gmail.com

How to cite this paper: Chaudhary, R.P., Hussain, M.M., Roy, N.K., Mandal, J. and Jha, I.S. (2026) Thermophysical Properties of InTl Melts at 723 K. *World Journal of Condensed Matter Physics*, **16**, 73-89.
https://doi.org/10.4236/wjcmp.2026.163005

Received: June 22, 2026
Accepted: August 28, 2026
Published: August 31, 2026

Abstract

The statistical mechanical model like self-association model (SAM) is taken into consideration to analyze the thermophysical properties of InTl melts at 723 K. The analytical expressions worked out in the light of SAM model are used to compute the thermodynamic and microscopic properties of InTl melts at 723 K. Again, Butler model and Moelwyn-Hughes model in conjunction with SAM model are employed to explore the concentration dependence of the surface as well as transport properties respectively for InTl melts at 723 K. The theoretical data of the thermophysical properties for InTl melts at 723 K exhibit well harmony with the correlated experimental data found in the literature. The results refer to the segregating nature of InTl melts at 723 K.

Keywords

SAM Model, Concentration Fluctuations, Free Energy of Mixing, Enthalpy of Mixing, Surface Tension and Transport Properties

1. Introduction

The In-Tl system represents a shape-memory alloy [1] possessing low melting point *i.e.* 578 K [2] which is less than that of pure In (*i.e.* 702.76 K) and Tl (*i.e.* 800 K). Again, In-Tl system has potential applications in metallurgy, thermostats, electric circuits, hydraulic lines, etc. [3]. The mixing properties of In-Tl molten alloys exhibit interesting behavior, *i.e.* the excess free energy of mixing, G_M^{XS}, entropy of mixing, S_M and free energy of mixing, G_M are symmetric while heat of mixing, H_M is asymmetric about $C = 0.5$ for InTl melts at 723 K [2]. The activity,

$a_i\left(i \equiv In, Tl\right)$ shows positive departures from linearity confirming that InTl melts at 723 K is a demixing alloy *i.e.* segregating alloy [4]. Thus, the structure and thermophysical properties of InTl melts have drawn attention of several investigators [1] [3] [5]. In the past, the thermophysical properties like diffusivity ratio, $\frac{D_M}{D_{id}}$, viscosity, η, G_M and concentration fluctuations, $S_{CC}\left(0\right)$ have been investigated [3] by quasi-lattice theory [4]. In quasi-lattice theory, the size effect *i.e.* size ratio of the constituent atoms, is coupled with the entropic and enthalpic effects to explain the thermodynamics of molten binary alloys and hence two model parameters namely size ratio and interaction energy are utilized to investigate the thermodynamic properties of the alloys. The simple statistical model [6] has been applied to study the segregating nature of InTl melts at 723 K [5] in terms of thermodynamic properties like G_M, a_i, S_M and H_M; microscopic properties like $S_{CC}\left(0\right)$ as well as short-range order parameter, α_1; surface properties like surface concentration, C_i^s as well as surface tension, σ and transport properties like $\frac{D_M}{D_{id}}$ and η for InTl melts at 723 K. In simple statistical model, the entropic and enthalpic effects are utilized to explain the thermodynamics of binary molten alloys on assuming the constituent atoms are comparable in size (volume) and hence there is only one model parameter, known as interaction energy. However, the study of the stability function and surface concentration fluctuations $S_{CC}^s\left(0\right)$ of InTl melts at 723 K is not available in the literature. It should be pointed out that for InTl system, the size factor ($V_{Tl}/V_{In}=1.074$ *i.e.* $V_{Tl}\sim V_{In}$) and electronegativity difference (*i.e.* $E_{Tl}-E_{In}=1.8-1.7=0.1$) are small to account for the mixing properties of the alloy. The potential applications as shape memory alloys in medical devices, robotics etc., as well as the interesting properties of mixing ensure that InTl system is very crucial for the further theoretical investigation. Thus in present investigation, the theoretical explanation of the thermophysical properties of InTl melts is taken into account in the framework of self-association model. In this model, the size (*i.e.* volume) of the constituent atoms of the binary alloy is supposed to be comparable. Again, it is assumed that the atoms of the constituent elements form like-atoms clusters or self-associates. Therefore, the present model has two important parameters like ratio of number of two atoms in the self-associates and the interaction energy [4].

The self association model *i.e.* SAM [4] is employed to describe the thermodynamic functions like G_M, G_M^{XS}, a_{In} and a_{Tl}, S_M and H_M; and microscopic functions like $S_{CC}\left(0\right)$ well as α_1 and stability *i.e.* stability function, E^{XS} for InTl melts at 723 K. Again, Butler model [7] in the framework of SAM is employed to analyze surface properties like C_i^s, σ and $S_{CC}^s\left(0\right)$ for InTl melts at 723 K. Further, the Moelwyn-Hughes formula [8] is used in the light of SAM model to explain the transport properties like $\frac{D_M}{D_{id}}$ and η for InTl melts at 723 K. In the past, SAM model is successfully used to analyze the thermophysical properties of several alloys like GaSn, AlSn, FeSn, CdGa, AlTl, ZnCd, BiSn, GaZn,

etc. [9]-[14].

2. Formalism

In the substructure of SAM [4], the required equations are formulated for the bulk properties namely G_M^{XS}, G_M, a, H_M, S_M, $S_{CC}(0)$ as well as α_1 for a binary melt at a specified temperature. Again, the analytical expressions for the surface properties like C_i^s, σ and $S_{CC}^s(0)$ for a binary solution are developed by Butler model [7] in conjunction with SAM model. Further, the expressions for transport properties namely diffusivity, D as well as viscosity, η are deduced using Moelwyn-Hughes model [8] in the framework of SAM model for a binary solution.

2.1. Bulk Properties: Thermodynamic and Microscopic Properties of Binary Liquid Alloys

A binary system, A-B is supposed to be consisted of $N_A = NC_A$ as well as $N_B = NC_B$ atoms of metal A and metal B respectively where $C_A = C$ and $C_B = 1 - C$ denote the concentrations of constituents A and B, respectively. In SAM model, it is considered that the atoms are situated on equivalent lattice sites with Z nearest neighbors. The effective interactions are short-ranged and exist only between nearest neighbors. Further, consider that sizes of A and B are comparable and there exist like-atom clusters or self-associates like A_i and B_j so that

$$i\mathrm{A} \rightleftharpoons \mathrm{A}_i, j\mathrm{B} \rightleftharpoons \mathrm{B}_j \tag{1}$$

where i and j = number of atoms in self-associates types A and type B matrices respectively.

In SAM model [4] assuming $Z \to \infty$ [15], the expression for G_M is given by

$$\frac{G_M}{RT} = C_A \ln C_A + C_B \ln C_B + C_A \ln(1-\beta) + \ln\gamma + C_A C_B \gamma \frac{W}{RT} \tag{2}$$

where,

$$\beta = 1 - \frac{1}{n} \quad \text{and} \quad \gamma = \frac{1}{1 - C_A\beta} \tag{3}$$

with R and T = universal gas constant and absolute temperature respectively, $W = i\omega$, denotes interchange energy while $n = \frac{j}{i}$, $(j > i)$, ratio of number of two atoms in self-associates. It is pointed out that n and W are independent of composition and dependent on the pressure and temperature.

The equation of activity [4] for a binary melt is represented by

$$RT \ln a_A = G_M + C_B \left(\frac{\partial G_M}{\partial C_A} \right) \tag{4a}$$

$$RT \ln a_B = G_M + C_A \left(\frac{\partial G_M}{\partial C_B} \right) \tag{4b}$$

Equations (2) and (4) provide

$$\ln a_A = \ln\left(C_A\gamma\right) + \ln\left(1-\beta\right) + C_B\gamma\beta + C_B^2\gamma^2\frac{W}{RT} \tag{5}$$

$$\ln a_B = \ln\left(C_B\gamma\right) - C_A\gamma\beta + \left(1-\beta\right)C_A^2\gamma^2\frac{W}{RT} \tag{6}$$

Again, S_M for a binary melt is represented by [4]

$$S_M = -\left(\frac{\partial G_M}{\partial T}\right)_P \tag{7}$$

Equations (2) and (7) provide

$$\begin{aligned}\frac{S_M}{R} = &-C_A\ln C_A - C_B\ln C_B - C_A\ln\left(\frac{1}{n}\right) - \ln\gamma - C_AC_B\gamma\frac{1}{R}\frac{\partial W}{\partial T}\\ &+ TC_AC_B\gamma\left(\frac{\beta}{1-\beta} - C_A\gamma\frac{W}{RT}\right)\frac{\partial\beta}{\partial T}\end{aligned} \tag{8}$$

where, $\frac{\partial W}{\partial T}$ = temperature derivative of W.

The H_M for a binary melt is expressed as

$$H_M = G_M + TS_M$$

Equations (2), (8) and (9) provide

$$\frac{H_M}{RT} = C_AC_B\gamma\frac{W}{RT} - C_AC_B\gamma\frac{1}{R}\frac{\partial W}{\partial T} + TC_AC_B\gamma\left(\frac{\beta}{1-\beta} - C_A\gamma\frac{W}{RT}\right)\frac{\partial\beta}{\partial T} \tag{9}$$

The structural functions like $S_{CC}\left(0\right)$ [16] and α_1 [17], [18] are very useful microscopic functions for acquiring the knowledge of the nature as well as degree of local arrangement of atoms in the binary melts. The $S_{CC}\left(0\right)$ and G_M are related as [16]

$$S_{CC}\left(0\right) = RT\left[\frac{\partial^2 G}{\partial C^2}\right]^{-1}_{T,P,N} \tag{10}$$

Expressions (2) and (10) yield

$$S_{CC}\left(0\right) = \frac{C_AC_B}{1-C_AC_Bf\left(n,W\right)} \tag{11}$$

where,

$$f\left(n,W\right) = \frac{2n^2\frac{W}{RT} - \left(n-1\right)^2\left(C_A+nC_B\right)}{\left(C_A+nC_B\right)^3} \tag{12}$$

For $f\left(n,W\right)=0$, expression (12) reduces to

$$S_{CC}^{id}\left(0\right) = C_AC_B = C\left(1-C\right) \tag{13}$$

which represents the ideal value of $S_{CC}\left(0\right)$.

The activity and $S_{CC}\left(0\right)$ are related as [16]

$$S_{CC}\left(0\right) = Ca_AC_B\left[\frac{\partial a_A}{\partial C_A}\right]^{-1}_{T,P,N} = a_BC_A\left[\frac{\partial a_B}{\partial C_B}\right]^{-1}_{T,P,N} \tag{14}$$

The Equation (14) provides the experimental data of $S_{CC}\left(0\right)$ for the binary

melts if the experimental data for a_A and a_B are utilized.

Again, α_1 in the nearest-neighbor shell for a binary melt [4], [17], [18] and $S_{CC}(0)$ are related as

$$\alpha_1 = \frac{(S-1)}{S(Z-1)+1} \quad \text{with} \quad S = \frac{S_{CC}(0)}{S_{CC}^{id}(0)} \tag{15}$$

where, Z denotes the coordination number, which is taken to be 10.

The $S_{CC}(0)$ is an important parameter used to describe the stability of a binary melt. In terms of $S_{CC}(0)$, excess stability function, E^{XS} [19] is represented by [4], [20], [21]

$$E^{XS} = \frac{\partial^2 G_M}{\partial C^2} - \frac{RT}{C(1-C)}$$

$$\frac{E^{XS}}{RT} = \frac{1}{S_{CC}(0)} - \frac{1}{S_{CC}^{id}(0)} \tag{16}$$

2.2. Surface Properties of Binary Liquid Alloys

The properties like C_i^s, σ as well as surface concentration fluctuations, $S_{CC}^s(0)$ describe the characteristics like energy of phase alternation, mechanical behavior, thin film, etc. Hence, the present investigation is concerned with the study of the surface properties of binary melts by Butler model [7].

According to Butler model [7], the surface tension, σ of a binary melt is expressed as

$$\sigma = \sigma_A + \frac{\tilde{G}_A^{E,s} - \tilde{G}_A^{E,b}}{S_A} + \frac{RT}{S_A}\ln\left(\frac{C_A^s}{C_A}\right) \tag{17a}$$

$$\sigma = \sigma_B + \frac{\tilde{G}_B^{E,s} - \tilde{G}_B^{E,b}}{S_B} + \frac{RT}{S_B}\ln\left(\frac{C_B^s}{C_B}\right) \tag{17b}$$

where, $\sigma_i (i = A, B)$ = surface tension of i^{th} component in molten state, $\tilde{G}_i^{E,s}$ = partial excess free energy at the surface for component i, $\tilde{G}_i^{E,b}$ = partial excess free energy in the bulk for component i, $S_i (i \equiv A, B)$ = molar surface area of i^{th} component, and C_i^s and C_i = surface and bulk compositions respectively. Now, $S_i (i \equiv A, B)$ may be expressed as [9]

$$S_i = 1.09 V_i^{\frac{2}{3}} N_A^{\frac{1}{3}} \tag{18}$$

where, V_i = atomic volume of component i, N_A = Avogadro's number.

Now, the expression for $\tilde{G}_i^{E,b}$ is given by [4]

$$\tilde{G}_i^{E,b} = RT \ln \gamma_i \tag{19}$$

where, γ_i = activity coefficient of i^{th} component.

Again, $\tilde{G}_i^{E,b}$ and $\tilde{G}_i^{E,s} (i \equiv A, B)$ are related as [22]

$$\tilde{G}_i^{E,s} = \lambda \tilde{G}_i^{E,b} \tag{20}$$

with, $\lambda = \frac{Z^S}{Z}$ [23] where Z^S = surface coordination number and Z = bulk

coordination number. It is necessary to proclaim that the value of λ lies between 0.50 to 0.84 [24]. In present study, the value of λ is taken to be 0.818 [25].

Now, $S_{CC}^{s}(0)$ which deals with the arrangement of atoms at the surface of binary solution. The expression for $S_{CC}^{s}(0)$ is given by [26]

$$S_{CC}^{s}(0)=\frac{C_A^s C_B^s}{1+\frac{Z^S}{2\lambda^S}\left(1-\lambda^S\right)} \tag{21}$$

with,

$$\lambda^S=\left[1+4C_A^S C_B^S\left(\mathrm{e}^x-1\right)\right]^{\frac{1}{2}} \tag{22}$$

where,

$$x=\frac{2W}{Z^s K_B T} \tag{23}$$

and

$$Z^S=\lambda Z \tag{24}$$

The ideal $S_{CC}^{s}(0)$ is represented by [26]

$$S_{CC}^{s,id}(0)=C_A^S C_B^S \tag{25}$$

2.3. Transport Properties of Binary Liquid Alloys

The diffusivity ratio and $S_{CC}(0)$ is related as [4], [14]

$$\frac{D_M}{D_{id}}=\frac{S_{CC}^{id}(0)}{S_{CC}(0)} \tag{26}$$

where, D_M denotes the mutual diffusion coefficient while D_{id} represents the intrinsic diffusion coefficient of an ideal mixture.

Again, D_{id} is represented by

$$D_{id}=C_A D_B+C_B D_A \tag{27}$$

where, D_A and D_B = self-diffusion coefficients of pure elements A and B respectively.

The viscosity is helpful to explain the interatomic interactions between the elements of a binary melt. From Moelwyn-Hughes approach [8], η can be expressed as

$$\eta=\eta_{id}\left[1-C_A C_B\left(\frac{2\omega}{K_B T}\right)\right] \tag{28}$$

where, η_{id} = viscosity of the ideal melt which is represented as

$$\eta_{id}=C_A\eta_A+C_B\eta_B \tag{29}$$

where, η_A and η_B = viscosities of pure elements A and B respectively.

Now, H_M may be represented by [4]

$$\frac{H_M}{RT}=-C_A C_B\frac{\omega}{K_B T} \tag{30}$$

Equations (28) and (30) provide

$$\eta = \left(C_A\eta_A + C_B\eta_B\right)\left(1 - 2\frac{H_M}{RT}\right) \tag{31}$$

Equation (31) indicates that η depends upon the magnitude of $\frac{H_M}{RT}$.

3. Results and Discussions

The analytical expressions are employed to compute the thermophysical properties of InTl melts at 723 K.

3.1. Bulk Properties: G_M^{XS}, G_M, a, H_M, S_M, $S_{CC}(0)$, α_1 and E^{XS} for InTl Melts at 723 K

The model parameters like n and W are required for the theoretical investigation of the bulk properties of InTl melts at 723 K. The values of n and W are estimated by the method of successive approximation approach [11], [13], [14] on taking the experimental data of G_M [2] in Equation (2) for InTl melts at 723 K. The suitable values are

$$n = 1.081 \quad W = 0.491RT$$

The theoretical data for $\frac{G_M}{RT}$ of InTl melts at 723 K are presented in **Figure 1** along with the correlated experimental data [2] relative to the composition of In which displays well agreement in the whole composition region of In, $C_{In} = 0.1$ to 0.9. The values of $\frac{G_M}{RT}$ are negative in the whole composition range with minima at $C_{In} = 0.5$ *i.e.* $\frac{G_M}{RT}\left(\min^m\right) = -0.5664$ (Theory) and −0.5669 (Experiment). Thus, the symmetry in G_M for InTl melts at 723 K is well explained theoretically.

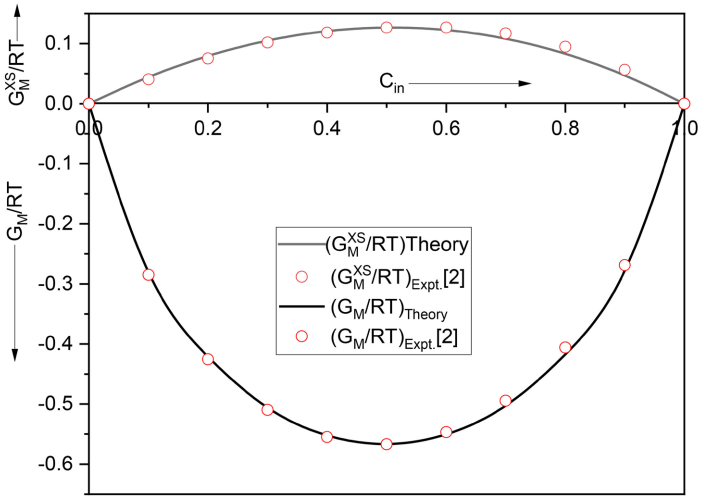

Figure 1. $\frac{G_M^{XS}}{RT}$ and $\frac{G_M}{RT}$ versus C_{In} for InTl melts at 723 K.

The G_M^{XS} for InTl melts at 723 K is computed by the relation

$$\frac{G_M^{XS}}{RT}=\frac{G_M}{RT}-\frac{G_M^{id}}{RT}=\frac{G_M}{RT}-\left(C_A\ln C_A+C_B\ln C_B\right) \tag{32}$$

A well agreement is observed between theory and experiment [2] for G_M^{XS} of InTl melts at 723 K as depicted in **Figure 1**. The positive values of G_M^{XS} are found in whole region, $C_{In}=0.1$ to 0.9 having maxima *i.e.* $\frac{G_M^{XS}}{RT}\left(\max^{m}\right)=0.1268$ (Theory) and 0.1267 (Experiment) both at $C_{In}=0.5$. Hence, the symmetry in G_M^{XS} for InTl melts at 723 K is explained satisfactorily. Again, the magnitude as well as sign of $\frac{G_M^{XS}}{RT}$ reveal that InTl melts at 723 K is a feebly segregating alloy [4].

Now, the activities a_{In} and a_{Tl} of In and Tl respectively, computed via Equations (5) and (6) are displayed in **Figure 2** along with the corresponding experimental results [2] for InTl melts at 723 K. An excellent harmony is noticed. Again, the small positive departures from Raoult's law are noticed for a_{In} and a_{Tl} in the complete composition range *i.e.* $C_{In}=0.1$ to 0.9, which signifies the feebly segregating nature [4] of InTl melts at 723 K. Thus, the well agreement between theory and experiment for a_{In} as well as a_{Tl} provides the authenticity of the evaluated values of n and W.

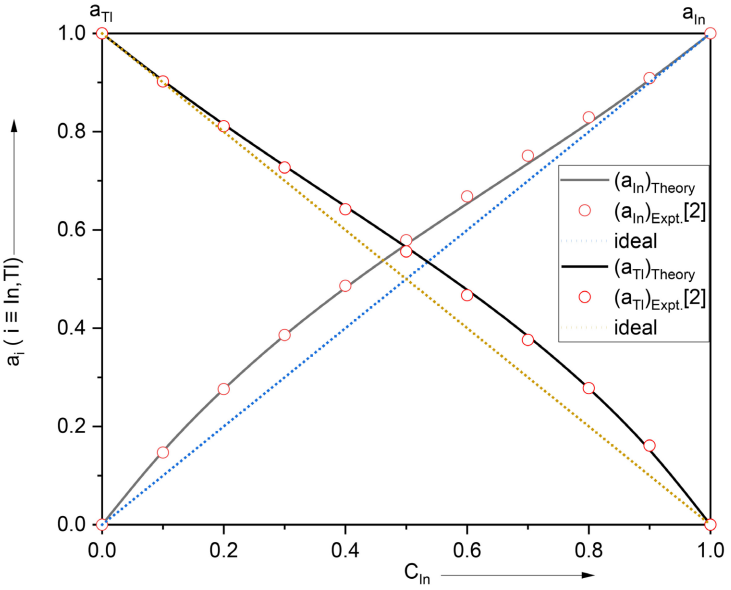

Figure 2. $a_i\left(i=In,Tl\right)$ versus C_{In} for InTl melts at 723 K.

For the computations of S_M and H_M for InTl melts 723 K via Equations (8) and (9), the values of $\frac{\partial\beta}{\partial T}$ and $\frac{\partial W}{\partial T}$ are required. The evaluated values of $\frac{\partial\beta}{\partial T}$ and $\frac{\partial W}{\partial T}$ by least square method [13], [14] on employing the experimental values of S_M [2] in expression (8) are -1×10^{-5} K^{-1} and 0.333 R, respectively.

Figure 3 shows the comparison between the theoretical result of S_M determined from Equation (8), and the correlated experimental data [2] for InTl melts at 723 K and exhibits excellent agreement in the region, $C_{In}=0.1$ to 0.9. The peak values are observed at $C_{In}=0.5$ *i.e.* $\frac{S_M}{R}\left(\max^{m}\right)=0.6595$ (Theory) and 0.6596 (Experiment). This successfully reproduces the symmetry in S_M for InTl melts at 723 K.

Again, the theoretical values of H_M in terms of the composition of In for InTl melts at 723 K, computed from Equation (9) are in reasonable agreement with the corelated experimental data [2] as mentioned in **Figure 3**. However, a minor discrepancy is noticed *i.e.* $\frac{H_M}{RT}\left(\max^{m}\right)=0.093$ (Theory) at $C_{In}=0.55$ and 0.0947 (Experiment) at $C_{In}=0.6$, which shows the asymmetric behaviour of InTl melts at 723 K. Further, the values of H_M are positive in the complete composition region of In, which indicates the demixing nature of InTl melts at 723 K [4].

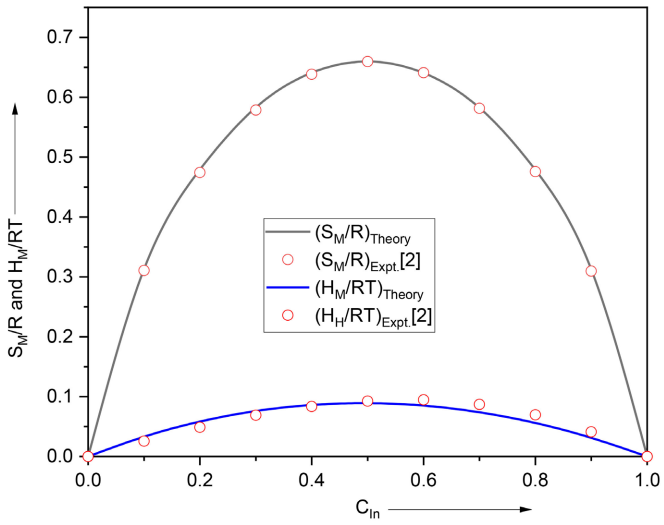

Figure 3. $\frac{S_M}{R}$ and $\frac{H_M}{RT}$ versus C_{In} for InTl melts at 723 K.

The theoretical data of $S_{CC}(0)$ for InTl melts at 723 K in terms of composition of In, computed via Equations (11) and (12) are mentioned in **Figure 4**. The experimental data of $S_{CC}(0)$ [2] and ideal $S_{CC}(0)$ are also displayed in **Figure 4**. A well agreement is noticed between theory and experiment with some departures in the region $0.4 \le C_{In} \le 0.6$ so that maximum error is about 5.38% at $C_{In}=0.5$. In the complete range of composition, $0.0 \le C_{In} \le 1.0$, $S_{CC}(0) > S_{CC}^{id}(0)$ having the peak values of 0.315 (Theory) and 0.318 (Experiment) both at $C_{In}=0.5$. This advocates the segregating nature of InTl melts at 723 K [4]. Further, the difference between the peak values of $S_{CC}(0)$ and $S_{CC}^{id}(0)$ *i.e.* $S_{CC}(0)-S_{CC}^{id}(0)$ for InTl melts at 723 K is found to be 0.085 which is very close to 0.0846 as available in the literature [3].

Equation (15) is utilized to compute the values of α_1 relative to the

composition of In for InTl melts at 723 K. Figure 4 also displays the $\alpha_1 - C$ isotherm for InTl melts at 723 K. It should be pointed out that no experimental data of α_1 for InTl melts at 723 K are available in the literature for comparison. It is obvious from Figure 4 that α_1 is positive at each composition throughout the composition range of In form 0.1 to 0.9. The sign and magnitude of α_1 indicate that InTl melt is a feebly segregating alloy.

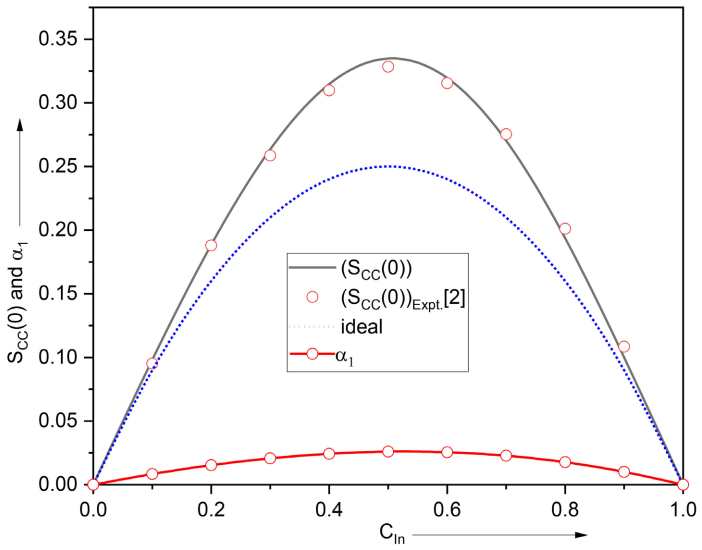

Figure 4. $S_{CC}(0)$ and α_1 versus C_{In} for InTl melts at 723 K.

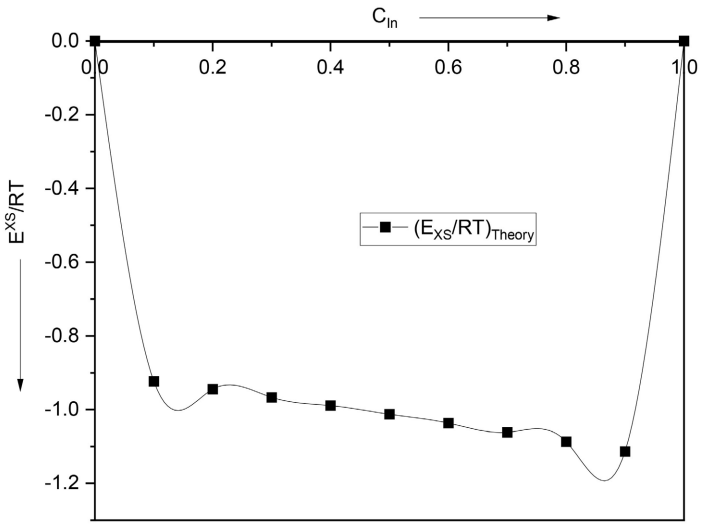

Figure 5. $\frac{E^{XS}}{RT}$ versus C_{In} for InTl melts at 723 K.

The excess stability function is useful to study the nature of atomic interactions in a binary melt. The negative value of E^{XS} signifies the segregating nature of binary melts because in this case, $S_{CC}(0) > S_{CC}^{id}(0)$. Similarly, E^{XS} becomes positive for ordered alloys due to $S_{CC}(0) < S_{CC}^{id}(0)$ [4]. The theoretical values of

$S_{CC}(0)$ are utilized in Equation (16) to explain the concentration dependence of E^{XS} for InTl melts at 723 K. Figure 5 displays the $\frac{E^{XS}}{RT}-C$ isotherm for InTl melts at 723 K. Obviously, InTl melt at 723 K represents the segregating behaviour because its value is negative in the complete composition region of In *i.e.* $C_{In}=0.1$ to 0.9. Again, the magnitude of the negative values of $\frac{E^{XS}}{RT}$ advocates the weakly segregating nature of InTl melts at 723 K.

3.2. Surface Properties: C_{In}^{s}, σ and $S_{CC}^{s}(0)$ for InTl Melts at 723 K

The simultaneous solution of Equations (17a) and (17b) provides the values of C_{In}^{s} and σ relative to the bulk concentration of In *i.e.* C_{In}^{b} $(=C_{In})$. The necessary parameters are evaluated from Equations (18), (19) and (20). The values of σ for pure In and pure Tl at 723 K are achieved from the expression given below

$$\sigma_i(T)=\sigma_i(T_m)+\frac{\partial\sigma_i}{\partial T}(T-T_m)\quad (i=In,Tl) \tag{33}$$

where, $T=723$ K.

T_m = melting temperature;

$\sigma_i(T)$ = surface tension of molten component i in pure state at T K;

$\sigma_i(T_m)$ = surface tension of pure component i at T_m K;

$\frac{\partial\sigma_i}{\partial T}$ = derivative of surface tension for i^{th} component with respect to temperature.

The values of input parameters are incorporated in Table 1 [27].

Table 1. Surface tension and temperature coefficient of surface tension for Tl and In [27].

Metal	Melting point T_m (K)	Surface tension (σ in mN·m^{-1})	Temp$^{r.}$ coefficient of surface tension ($\frac{\partial\sigma}{\partial T}$ in mN·m^{-1}·K^{-1})
In	429.55	556	−0.09
Tl	575.65	464	−0.08

The values of σ_{In} and σ_{Tl} at 723 K are found to be 529.590 mN·m^{-1} and 452.212 mN·m^{-1}, respectively.

The values of V_i $(i=In,Tl)$ for pure components *i.e.* In and Tl at 723 K, are determined from the equations given below

$$V_i(T)=\frac{M_i}{\rho_i(T)} \tag{34a}$$

with

$$\rho_i(T)=\rho_i(T_m)+\frac{\partial\rho_i}{\partial T}(T-T_m)\quad (i\equiv In,Tl) \tag{34b}$$

where,

$\rho_i(T)$ = density of the i^{th} component at 723 K;

$\rho_i(T_m)$ = density of the i^{th} component at melting temperature;
M_i = atomic mass of the i^{th} component;
$\frac{\partial \rho_i}{\partial T}$ = temperature coefficient of the density for the i^{th} component.
The required physical quantities are presented in **Table 2** [27].

Table 2. Data for the physical properties of In and Tl [27].

Metal	M.P. (T_m in K)	Atomic mass (M in Kg)	Density (ρ in Kg·m^{-3})	Temp^r. Coefft. of Density ($\frac{\partial \rho}{\partial T}$ in Kg·m^{-3}·K^{-1})
In	429.55	0.11482	7030	−0.68
Tl	575.65	0.20437	11350	−1.30

The theoretical values of C_{In}^s relative to the bulk concentration of In *i.e.* C_{In} are depicted in **Figure 6**. It is clear that C_{In}^s rises when the bulk composition of In increases. Again, in the complete composition range of In, $C_{In} = 0.1$ to 0.9, C_{In}^s denotes the negative deviation from linearity which advocates that atoms of Tl segregate on the surface for InTl melts at 723 K.

Figure 7 displays the theoretical values of σ in terms of the bulk composition of In for InTl melts at 723 K. Obviously, the value of σ increases when concentration of In increases from 0.0 to 1.0. This arises due to the fact that pure In has larger value of surface tension than pure Tl.

Now, equations (21) and (22) are utilized to study the composition dependency of $S_{CC}^s(0)$ relative to the bulk composition of In for InTl melts at 723 K. The theoretical result is illustrated in **Figure 8** along with the ideal values of $S_{CC}^s(0)$. Obviously, $S_{CC}^s(0)$ exhibits positive deviation from $S_{CC}^{s,id}(0)$ in the entire bulk composition of In. The $S_{CC}^s(0)$ has maximum value of 0.3301 at $C_{In} = 0.7$ which indicates the maximum possibility of phase separation in InTl melts at 723 K close to $C_{In} = 0.7$ [13].

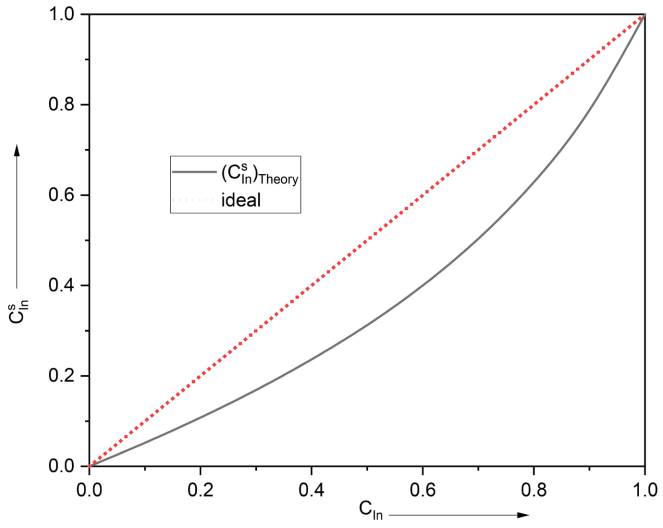

Figure 6. C_{In}^s versus C_{In} for InTl melts at 723 K.

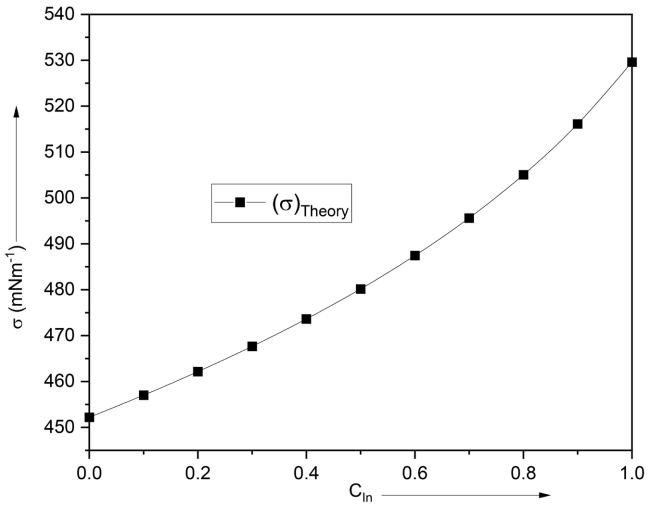

Figure 7. σ versus C_{In} for InTl melts at 723 K.

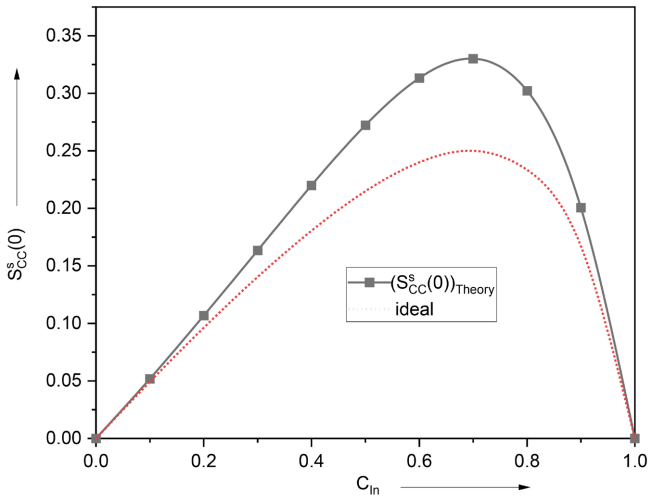

Figure 8. $S_{CC}^{s}(0)$ versus C_{In} for InTl melts at 723 K.

3.3. Transport Properties: $\frac{D_M}{D_{id}}$ and η for InTl Melts at 723 K

Figure 9 displays the theoretical values of $\frac{D_M}{D_{id}}$ relative to the composition of In for InTl melts at 723 K. For computations, the theoretical values of $S_{CC}(0)$ for InTl melts at 723 K are used in Equation (26). It is evident from **Figure 9** that $\frac{D_M}{D_{id}}$ is less than 1 in the complete composition region of In with the minimum value of 0.7468 at $C_{In}=0.5$, which is very close to 0. 7465 as available in the literature [5]. This indicates that $S_{CC}(0)$ is greater than $S_{CC}^{id}(0)$ in the region, $C_{In}=0.1$ to 0.9. The minimum value of $\frac{D_M}{D_{id}}$ shows that the InTl melt at 723 K is a weakly segregating alloy [28].

The computed data of $\frac{H_M}{RT}$ are employed to compute the values if η relative to the composition of In for InTl melts at 723 K. The values of η for pure In and pure Tl melts at 723 K are evaluated from the data available in the literature [29], which are found to be 0.9872 (mPa s) and 1.8678 (mPa s) respectively. **Figure 10** illustrates the composition dependency of η for InTl melts at 723 K in the region $0.0 \le C_{In} \le 1.0$. Obviously, the viscosity of InTl melts at 723 K declines with the elevation of bulk composition of In.

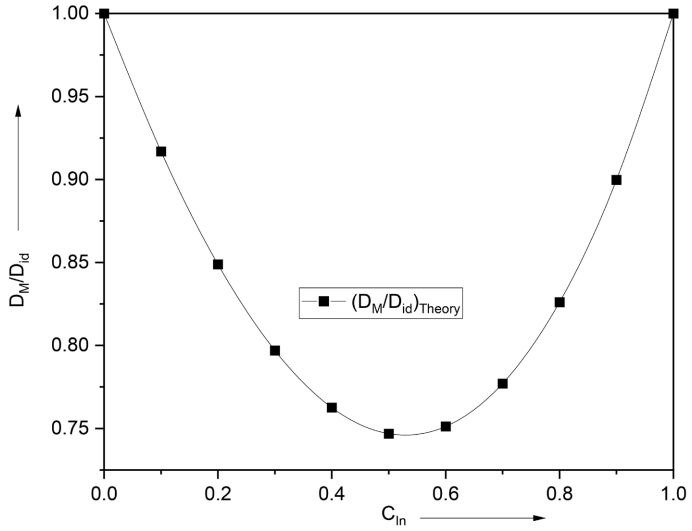

Figure 9. $\frac{D_M}{D_{id}}$ versus C_{In} for InTl melts at 723 K.

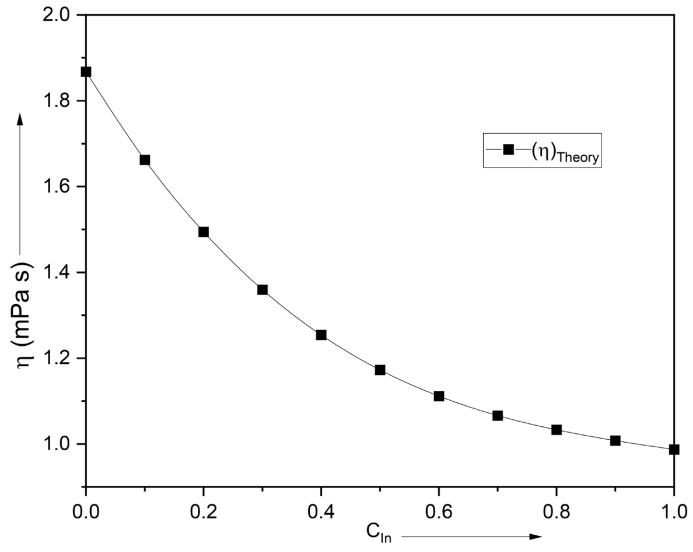

Figure 10. η versus C_{In} for InTl melts at 723 K.

4. Conclusions

The thermophysical properties of InTl melts at 723 K are successfully analyzed by

SAM model. The experimentally observed symmetries in G_M, G_M^{XS} and S_M as well as asymmetry in H_M are successfully analyzed. The composition dependency of G_M^{XS}, H_M, a_{In}, a_{Tl}, $S_{CC}(0)$, α_1, $\frac{D_M}{D_{id}}$, $S_{CC}^s(0)$, E^{XS} suggests that InTl melt at 723 K is a feebly segregating alloy. Again, the concentration dependence of C_{In}^s advocates that the atoms of Tl isolate at the surface for InTl melts at 723 K. For InTl melts at 723 K, the surface tension increases when bulk concentration of In increases.

Therefore, SAM model is a reliable and an appropriate model for the theoretical assessment of the demixing (or segregating) liquid alloys at a specified temperature. Further, the model may be employed to study the concentration dependence of the thermophysical properties of segregating molten alloys at various temperatures in the framework of optimization procedure. However, the present work has some limitations, such as scanty of experimental data and the application of self-association model in phase diagram calculations.

Author Contributions

Conceptualization: I.S. Jha and J. Mandal; methodology: R.P. Chaudhary; validation: I.S. Jha; J. Mandal and N.K. Roy; formal analysis: N.K. Roy; investigation: M.M. Hussain; writing-original draft preparation: M.M. Hussain; writing-review and editing: R.P. Chaudhary; visualization: I.S. Jha; supervision: J. Mandal.

Conflicts of Interest

The authors declare no conflicts of interest regarding the publication of this paper.

References

[1] Luo, Z.P. (2012) An Overview on the Indium-Thallium (IN-TL) Shape Memory Alloy Nanowires. *Metallography, Microstructure, and Analysis*, **1**, 320-326. https://doi.org/10.1007/s13632-012-0046-4

[2] Hultgren, R., Desai, P.D., Hawkins, D.T., Gleiser, M. and Kelley, K.K. (1973) Selected Values of the Thermodynamic Properties of Binary Alloys. ASM. American Society for Metals (ASM). Metal Park, OH.

[3] Awe, O.E. (2018) Thermodynamic Investigation of Thermophysical Properties of Thallium-Based Liquid Alloys. *Physics and Chemistry of Liquids*, **57**, 296-310. https://doi.org/10.1080/00319104.2018.1443453

[4] Singh, R.N. and Sommer, F. (1997) Segregation and Immiscibility in Liquid Binary Alloys. *Reports on Progress in Physics*, **60**, 57-150. https://doi.org/10.1088/0034-4885/60/1/003

[5] Koirala, I., Singh, B.P. and Jha, I.S. (2014) Theoretical Assessment on Segregating Nature of Liquid In-Tl Alloys. *Journal of Non-Crystalline Solids*, **398**, 26-31. https://doi.org/10.1016/j.jnoncrysol.2014.04.018

[6] Singh, R.N. and Mishra, I.K. (1988) Conditional Probabilities and Thermodynamics of Binary Molten Alloys. *Physics and Chemistry of Liquids*, **18**, 303-319. https://doi.org/10.1080/00319108808078606

[7] Butler, J.A.V. (1932) The Thermodynamics of the Surfaces of Solutions. *Proceedings*

of the Royal Society of London. Series A, Containing Papers of a Mathematical and Physical Character, **135**, 348-375. https://doi.org/10.1098/rspa.1932.0040

[8] Moelwyn-Hughes, E.A. (1961) Physical Chemistry, Pergamon Press.

[9] Anusionwu, B.C., Madu, C.A. and Orji, C.E. (2009) Theoretical Studies of Mutual Diffusivities and Surface Properties in Cd-Ga Liquid Alloys. *Pramana*, **72**, 951-967. https://doi.org/10.1007/s12043-009-0088-6

[10] Odusote, Y.A., Popoola, A.I. and Oluyamo, S.S. (2016) Bulk and Surface Properties of Demixing Liquid Al-Sn and Sn-Tl Alloys. *Applied Physics A*, **122**, Article No. 80. https://doi.org/10.1007/s00339-015-9591-4

[11] Awe, O.E. and Azeez, A.A. (2017) Temperature Dependence of the Bulk and Surface Properties of Liquid Zn-Cd Alloys. *Applied Physics A*, **123**, Article No. 363. https://doi.org/10.1007/s00339-017-0977-3

[12] Giuranno, D. and Novakovic, R. (2020) Surface and Transport Properties of Liquid Bi-Sn Alloys. *Journal of Materials Science: Materials in Electronics*, **31**, 5533-5545. https://doi.org/10.1007/s10854-020-03118-y

[13] Chaudhary, R.P., Mandal, J. and Indu Shekhar Jha, (2022) Symmetries in the Properties of Mixing of AgCu Liquid Alloys at 1423 K. *Materials Today: Proceedings*, **49**, 2283-2287. https://doi.org/10.1016/j.matpr.2021.09.343

[14] Chaudhary, R.P., Mandal, J. and Jha, I.S. (2022) Concentration Dependence of the Bulk and Surface Properties of Liquid AlZn Alloys at 1000K. *Materials Today: Proceedings*, **59**, 397-404. https://doi.org/10.1016/j.matpr.2021.11.358

[15] Guggenheim, E.A. (1952) Mixtures: The Theory of the Equilibrium Properties of Some Simple Classes of Mixtures, Solutions and Alloys. Oxford University Press.

[16] Bhatia, A.B. and Thornton, D.E. (1970) Structural Aspects of the Electrical Resistivity of Binary Alloys. *Physical Review B*, **2**, 3004-3012. https://doi.org/10.1103/physrevb.2.3004

[17] Warren, B.E. (1969) X-Ray Diffraction. Addition-Weseley.

[18] Cowley, J.M. (1950) An Approximate Theory of Order in Alloys. *Physical Review*, **77**, 669-675. https://doi.org/10.1103/physrev.77.669

[19] Darken, L.S. (1967) Thermodynamics of Binary Metallic Solutions. *Transactions of the Metallurgical Society of AIME*, **239**, 80.

[20] Singh, A.P., Chaudhary, R.P., Kumari, R., Jha, I.S. and Mandal, J. (2022) Stability of Nak Liquid Alloys at Different Temperatures. *Materials Today: Proceedings*, **66**, 2251-2258. https://doi.org/10.1016/j.matpr.2022.06.097

[21] Singh, A.P., Chaudhary, R.P., Hussain, M.M., Mandal, J. and Jha, I.S. (2024) Theoretical Study of the Stability of CdSn Liquid Alloy at Different Temperatures. *Diffusion Foundations and Materials Applications*, **37**, 37-51. https://doi.org/10.4028/p-efgqf5

[22] Plevachuk, Y., Sklyarchuk, V., Gerbeth, G., Eckert, S. and Novakovic, R. (2011) Surface Tension and Density of Liquid Bi-Pb, Bi-Sn and Bi-Pb-Sn Eutectic Alloys. *Surface Science*, **605**, 1034-1042. https://doi.org/10.1016/j.susc.2011.02.026

[23] Kaptay, G. (2005) A Method to Calculate Equilibrium Surface Phase Transition Lines in Monotectic Systems. *Calphad*, **29**, 56-67. https://doi.org/10.1016/j.calphad.2005.04.004

[24] Costa, C., Delsante, S., Borzone, G., Zivkovic, D. and Novakovic, R. (2014) Thermodynamic and Surface Properties of Liquid Co-Cr-Ni Alloys. *The Journal of Chemical Thermodynamics*, **69**, 73-84. https://doi.org/10.1016/j.jct.2013.09.034

[25] Kaptay, G. (2005) Modelling Interfacial Energies in Metallic Systems. *Materials Science Forum*, **473**, 1-10. https://doi.org/10.4028/www.scientific.net/msf.473-474.1

[26] Prasad, L.C. and Singh, R.N. (1991) Surface Segregation and Concentration Fluctuations at the Liquid-Vapor Interface of Molten Cu-Ni Alloys. *Physical Review B*, **44**, 13768-13771. https://doi.org/10.1103/physrevb.44.13768

[27] Iida, T. and Guthrie, R.I.L. (1988) The Physical Properties of Liquid Metals. Clarendon Press.

[28] Awe, O.E. (2016) The Role of Size Effect on the Bulk Properties of Copper-Tin Liquid Alloys. *Journal of Scientific Research*, **15**, 109-118.

[29] Hirai, M. (1993) Estimation of Viscosities of Liquid Alloys. *ISIJ International*, **33**, 251-258. https://doi.org/10.2355/isijinternational.33.251